

MULTI-LEVEL COMPUTER SIMULATION OF THE ENERGY SAVER COOLING PROVISIONS

H.R. Barton, Jr., G.T. Mulholland and J.E. Nicholls
 Fermi National Accelerator Laboratory*
 P.O. Box 500
 Batavia, IL 60510

Abstract

Mathematical models have been developed to describe the detailed temperature distributions within Energy Saver cryoloops as a function of static and ramp loads. The Satellite performance as a function of the Central Helium Liquefier flows, is calculated for a single equipment specification set. The performance of the system over a wide range of parameters results in clearly defined optima and detailed far-from-design predictions. The agreement of experimental test data and the simulation prediction is explored for individual magnets, magnet strings and the Satellite-mode refrigerator.

Introduction

The cryogenic system of the Fermilab Energy Saver consists of the Central Helium Liquefier, a nitrogen liquefier, and, distributed around the main ring, six Satellite helium compressor stations, 24 Satellite helium refrigerators, and 960 superconducting magnets. The system architecture provides a number of degrees of operating freedom and allows modular construction, at the expense of increased management complexity.

The purpose of the simulation is to systematically increase the depth of understanding at the component and system levels. Experience gained by operating the simulator is expanding the basis for management of the actual system.

A computer program was written to simulate the performance of the Satellite refrigerator. This program contains a mathematical model that can predict the effect of component variations, different operating modes, and system demands.

The refrigerator simulation provides the inlet boundary conditions to the magnet simulation: the time dependent model of a 20-magnet cryoloop that provides the cryoloop response to steady state, ramping, and transient loads.

Refrigerator Simulation

The Satellite refrigerator contains a heat-exchanger with a total UA of 14,000/°K at a flow of 40 g/s. The Satellite mode is the anticipated mode of operation during normal accelerator running. In this mode, the heat exchangers are unbalanced by liquid helium flow obtained from the Central Liquefier. If f is the high-pressure flow and F is the low-pressure flow, the flow imbalance is $\beta = 1 - f/F$. The Satellite also contains a wet-engine through which the high-pressure stream is expanded from 20 atm to 1.8 atm.

The heat-exchanger is constructed of coiled, finned tubing and the overall heat-transfer coefficient U is dominated by the effect of the tube h . The flow dependence is $j \sim (Re)^{-0.2}$ where $j = h (Pr)^{2/3} / (C_p G)$. The definitions are as follows: h = surface heat-transfer coefficient of the tube, G = mass flow per tube cross-sectional area, C_p = specific heat of helium, Pr = Prandtl number, Re = Reynolds number. This means

that UA of the heat exchanger increases with flow according to $UA \sim f^{0.8}$.

Figure 1 shows the calculated refrigeration available at the magnets using this model for the Satellite refrigerator. Lines labeled with values of β represent proportional changes in flow. The curvature of these lines is due to the decrease in effectiveness of the heat exchanger as flow increases.

Operation of the Satellite refrigerator at the lowest mass flow results in the lowest two-phase temperature at the magnets. The shell-side, pressure drop in the model is proportional to $F^{1.8}$. Figure 1 shows dashed isotherms; E-F is 4.4°K, G-H is 4.5°K and I-J is 4.6°K.

The Satellite refrigerators must provide liquid helium to cool the magnet power leads. Although the model accurately includes the calculation of the effect of providing lead flow, Figure 1 is the case where no lead flow is removed. The lead flow is 0.6 g/s per Satellite refrigerator in the average case. Non-zero lead flow increases the demand for helium from the Central Liquefier.

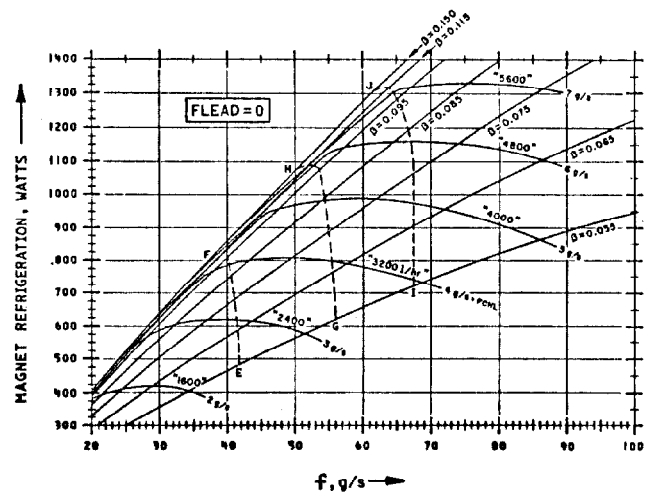


Figure 1. Magnet refrigeration provided as $F(\beta, f, F_{CHL})$.

Table I summarizes the requirements on the Central Liquefier. Ninety percent utilization of the Central Liquefier output is assumed in order to assure a continuous source of liquid helium to the 24th Satellite.

Table I

Central Helium Liquefier Requirements

		$f = 50 \text{ g/s}$	$\beta = 0.075$	0.085	0.095
FCHL (g/s)	{ FLEAD = 0		4.05	4.64	5.24
	{ FLEAD = 0.6 g/s		4.65	5.24	5.84
	{ @ 90% Utilization		5.17	5.82	6.49
24 Satellites (l/hr)			3,722	4,190	4,672

*Operated by Universities Research Assn., Inc., under contract with the U.S. Department of Energy.

Magnet Simulation

A Satellite refrigerator provides cooling to two parallel 20-magnet cryoloops. A single cryoloop is modeled with one-half Satellite flow; Figure 2 shows the relationship of these parts of the system. Figure 3 diagrams the 20-magnet string modeled here. Liquid helium flows to the magnet string through a subcooler at 1.8 atm, and is expanded at the far end to a lower pressure to return as two-phase liquid. The ramping heat load is deposited in the single-phase stream and is transferred to the colder two-phase counter-flow stream. The heat is primarily absorbed by the heat of vaporization of the two-phase fluid that returns to the Satellite through the shell side of the subcooler.

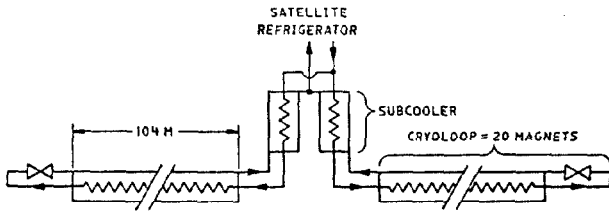


Figure 2. A Satellite drives parallel cryoloops.

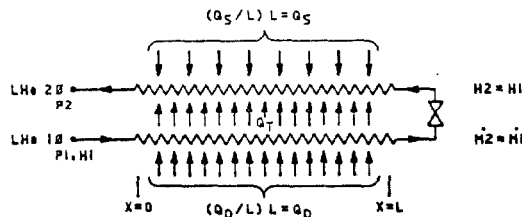


Figure 3. A cryoloop as a distributed heat exchanger.

Model

The cryoloop was simulated by simultaneous numerical solution of the one-dimensional mass, energy, and momentum conservation equations describing the helium streams, subject to appropriate boundary and initial conditions. The method follows that used by M.C. Jones¹ on superconducting power transmission lines, and uses the computer program PDECOL developed by N.K. Madsen and R.F. Sincovec² to integrate the partial differential equations.

There are a set of three equations for each stream, making six in all. The one-dimensional conservation equations are written in terms of pressure P , enthalpy H , and velocity V .³ The density ρ is a known function of P and H , and Λ is the heat transfer to the fluid per unit length. The friction factor is f , and p and a are the wetted perimeter and cross-sectional area of the channel.

$$\frac{\partial P}{\partial t} = -v \frac{\partial P}{\partial X} - \rho c^2 \frac{\partial v}{\partial X} + \phi \left[\frac{\Lambda}{a} + \rho \frac{v^2 f |v| p}{2a} \right]$$

$$\frac{\partial H}{\partial t} = -v \frac{\partial H}{\partial X} - c^2 \frac{\partial v}{\partial X} + \left(\frac{1+\phi}{\rho} \right) \left[\frac{\Lambda_1}{a} + \rho v^2 f |v| p \right]$$

$$\frac{\partial v}{\partial t} = -\frac{1}{\rho} \frac{\partial P}{\partial X} - v \frac{\partial v}{\partial X} - \frac{f v |v| p}{2a}$$

where the Gruniesen parameter ϕ and the acoustic velocity c , functions of the derivatives of ρ with respect to P and H , simplify the form. The necessary helium properties are parametrized as functions of P and H .⁴

The model is spatially uniform; the overall cross-sectional area, perimeter, heat inputs, and heat transfer coefficient are independent of X . The active portions of the magnet string have been modeled.

The boundary conditions selected fix the pressure of both streams and the enthalpy of the single-phase stream at the refrigerator end ($X=0$). The mass flow is fixed at the valve and the mass flow and enthalpy are continuous across it.

Initial conditions ($t=0$) must be provided for all values of X . The program is required to converge to a good steady state solution ($\partial(\)/\partial t \rightarrow 0$) as a starting point for the time-dependent studies.

The heat transfer to the fluid, Λ , is composed of two parts: the static load from heat leaks and the ramping load. The heat transfer from the single-phase stream to the two-phase stream is proportional to the temperature difference between the two streams and the heat transfer coefficient is a function of the geometry and materials. Although this coefficient does have some flow dependence, the average value used here provides a good approximation over the flow range studied.

The steady state case has been solved for an average anticipated load; average dynamic load, 250 watts, and 10 watts heat leak into the single-phase stream; and 140 watts of heat leak directly into the two-phase stream. The results are shown in Figure 4.

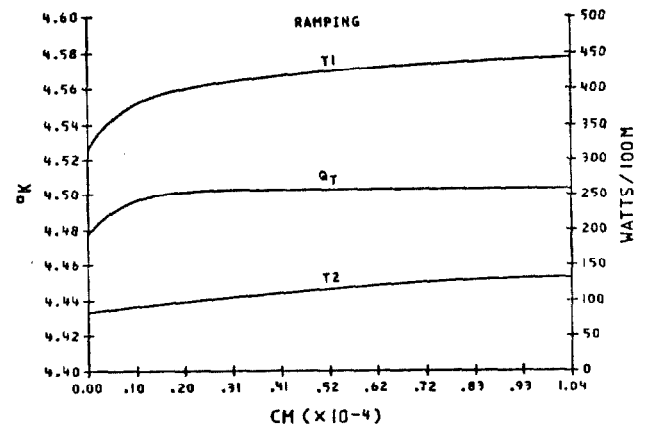


Figure 4. Steady state (dc). Q_T is heat transferred.

Ramping

The ramping current can be any $I(t)$ for which $Q(t) = F(I(t))$ is known. The ramp model used (200 A/sec, $I_{max} = 4000$ A, 5 sec flat top and 60 sec cycle time) closely parallels anticipated ramping (Figure 5). The load is taken to be proportional to $(\partial B / \partial t)^n$ and modified to one second rise and fall times for computational convenience. The resultant trapezoidal wave form has a peak of 375 W and an average of 250 W. The heat leak is the same as the steady state case.

The effect of ramping on the temperature is shown in Figure 6 at $X=0$, $L/2$, and L for two ramp cycles and both streams. Large values of $\partial T1 / \partial t$ have correspondingly large $\partial \rho / \partial t$ that provide velocities of expansion and contraction that subtract from, and add to, the transport velocity. The velocity of the single-phase fluid at $X=0$, $L/2$, and L are shown in Figure 7. Fixing the flow rate at the valve results in large variations at the refrigerator.

Ramp Off

The Saver Operations Group empirically demonstrated a cryoloop upset behavior caused by suddenly turning the ramp off. The magnet simulator was tested, in a preliminary way, to duplicate the observed behavior. The 250 watt dynamic load of the steady state case was reduced to zero in one second and the boundary conditions maintained.

The temperature distribution of the single-phase stream as a function of X at 20 second intervals is shown in Figure 8. The t=0 curve corresponds to the steady-state temperature distribution.

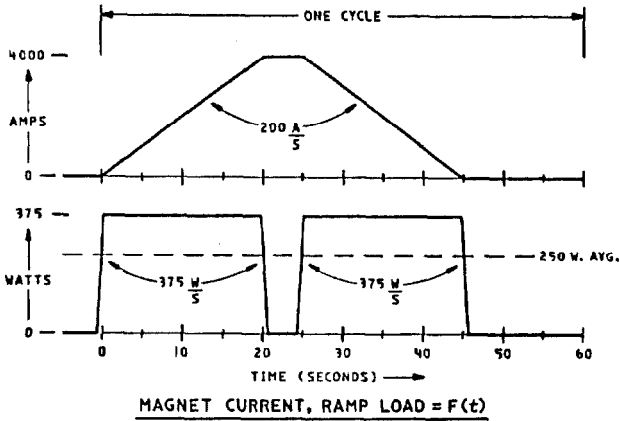


Figure 5. The ramping current and refrigeration load as function of time.

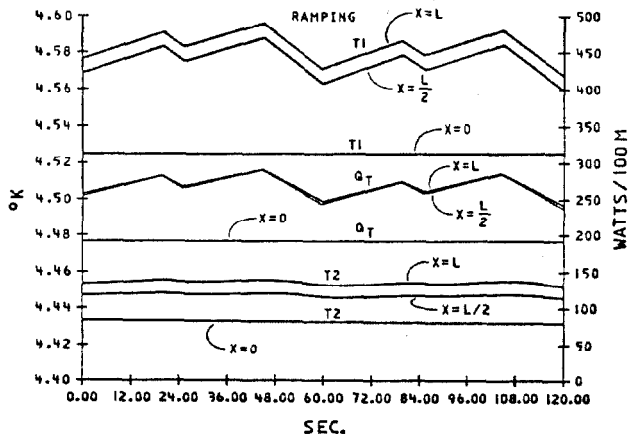


Figure 6. Heat transfer and single- and two-phase temperature; two cycles are shown.

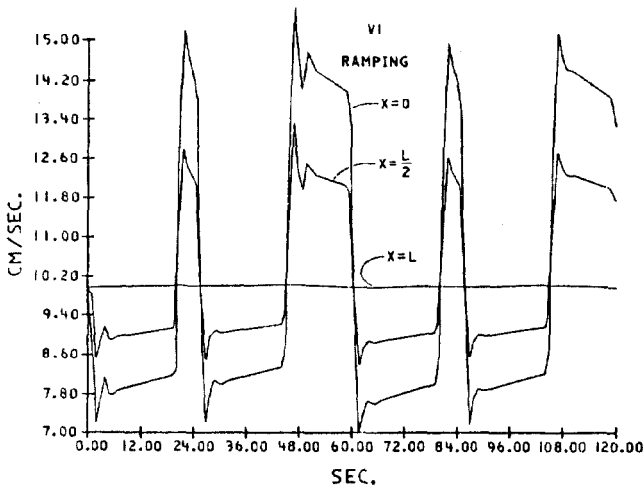


Figure 7. Velocity of single-phase over two cycles.

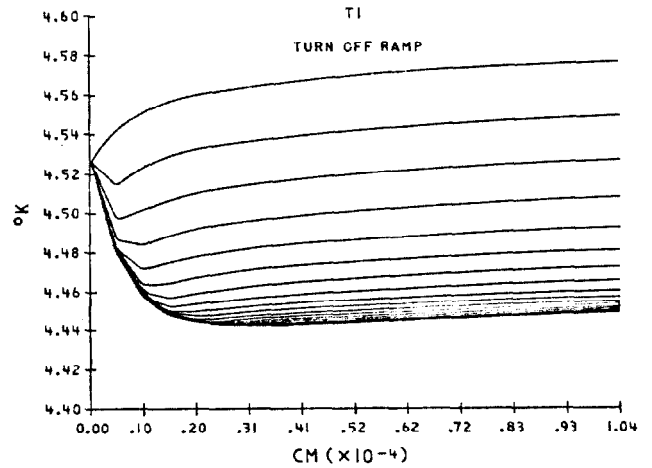


Figure 8. Single-phase temperature ramp turnoff.

The velocities of the single-phase stream at X=0, L/2, and L are shown versus time for 1200 seconds in Figure 9. These velocities have about the same value to a few percent at t=0.

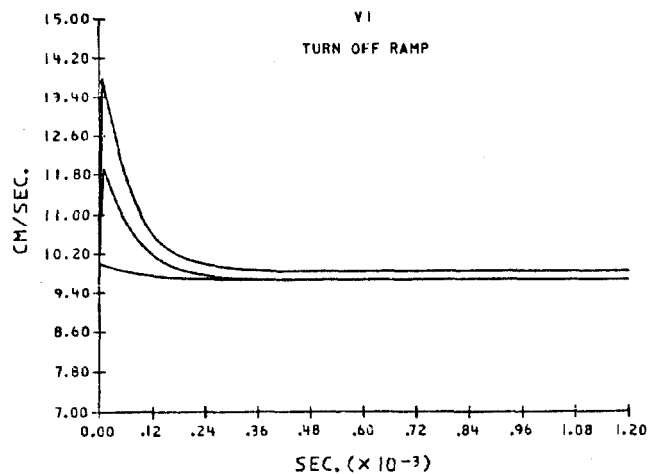


Figure 9. Ramp-off effect is virtually complete in four minutes.

References

1. Jones, M.C., Cryogenics, March 1980, p 139.
2. Madsen, N.K., Sincovec, R.F. in Numerical Methods for Differential Systems, L.Lapidus, W.E.Shiesser, ed., Academic Press, Inc., New York 1976.
3. Arp, V., Cryogenics, May 1975, p 285.
4. Arp, V., NBS, Boulder, CO, private communication.